Meander And Koch Hybrid Fractal Curve Based Dual Hexagonal Radiating Patch Antenna For Quad Band Wireless Applications

Jagtar Singh Sivia (jagtarsivian@gmail.com)
Punjabi University YCOE Talwandi Sabo
Sumeet Singh Bhatia
Yadavindra College of Engineering

Research Article

Keywords: Koch, Meander, Hybrid fractal, Patch antenna, Wi-MAX

Posted Date: July 13th, 2021

DOI: https://doi.org/10.21203/rs.3.rs-635399/v1

Abstract

A unique dual hexagonal-shaped radiating patch design with hybrid fractal curves (Meander and Koch) is presented for quad-band wireless applications. Initially, the antenna from 0th to 2nd iteration of hybrid fractal curves with PGP (Partial Ground Plane) is designed and investigated. Further, to get better results of the designed antenna in respect of Bandwidth (BW) and coefficient of reflection these hybrid curves are superimposed on the limited ground plane of 1st and 2nd iteration of the antenna, and the generated antennas are designated as Antenna – 1 and Antenna – 2. A comparison between both the antennas has been made and it is observed that antenna -2 shows better results in respect of improved BW and coefficient of reflection. The proposed antenna exhibits four resonant frequency bands 1.6, 4.8, 6.9, and 8.8GHz with improved corresponding impedance BW of 2.09, 1.36, 0.86, and 1.51GHz. The designed antenna is simulated and made on FR4 glass epoxy substrate with an overall size of 20×40×1.6 mm3. The fabricated proposed antenna is tested experimentally for the authentication of simulated results with experimental results and these are compatible with each other. The other performance indicators like radiation pattern, peak realized gain, and radiation efficiency are also determined for the proposed Hybrid Fractal Antenna (HFA) and all are found satisfactory. Due to the improved operational parameters, the designed HFA can be considered as a suitable applicant for distinct wireless applications in anticipated operational frequency ranges.

Introduction

In the recent moving age of wireless communication, numerous amendments are done in the field of antennas by eminent researchers to encounter the existing need of the marketplace. Basically, the antenna is a prime requirement of the various gadgets that are used by the individuals in their life, such as smartphones, laptops, smart televisions, i-pads, toys, wireless gaming equipment, etc. There is an excess of literature that has been presented that is linked to patch antennas but the fractal antenna has made its exceptional identity in the family of antennas because of its unusual features and capability to inhabit the huge surface area in restricted space [1, 2]. The fractal was first presented in 1975 by B. Mandelbrot on naturals fractals [3, 4]. Fractals are complicated in shape which occurs in nature or can be generated by means of IFS (Iterative Function System) [5, 6]. Fractals are based on distinct properties such as fractional proportions, space-filling, immeasurable complexity, and self–similarity due to which they exhibit wideband and multiband characteristics [7–9]. the utmost major properties of fractal shapes are self–similarity and space-filling. Space-filling property supports condense the overall antenna size known as miniaturization of antenna by refining the relative permittivity and permeability of substrate material [10, 11]. Whereas, another important property is beneficial to achieve the wideband/multiband characteristics [12, 13]. The shapes which are most commonly used in generating the fractal antennas are Koch [14–16], Minkowski [17–19], Sierpinski Gasket and Carpet [20–22], Hilbert [23–25], Giuseppe Peano [26–28], Meander [29–31], etc. All the discussed fractal shapes have their inimitable implication in the design of antennas for definite wireless standards. Antenna based on distinct fractal shapes is not able to attain multiband and wideband characteristics deprived of negotiating the operation of the

antenna. By keeping more attention on this problem, numerous researchers have attached these shapes together to project the different antennas for various wireless standards. These invented shapes are known as hybrid shapes and thus antennas obtained by applying these shapes are denoted as HFA (Hybrid Fractal Antenna). This can be generated by employing the different amalgamations as Koch-Koch, Meander-Meander, Koch-Meander, Koch-Sierpinski carpet/gasket, Sierpinski carpet/gasket-Giuseppe Peano, etc. In this document, a unique design of dual hexagonal patch is designed and the hybrid fractal shape of (Meander and Koch) has been superimposed on the construction of radiating patch to advance the presentation of the antenna in respect of coefficient of reflection, BW, and gain. Further, the hybrid curve has also been introduced on the PGP of the proposed shape of the antenna to attain wideband characteristics. The final shape of the proposed HFA has been made up and tested for the authentication of simulated and experimental results. The juxtaposition of these results shows that they are congruent with each other.

Antenna Design

2.1 HFA design evolution

This manuscript presents the design of a unique dual hexagonal patch antenna loaded with Koch and Meander hybrid fractal curve for quad-band wireless applications. The initial design of antenna begins with designing of the hexagonal radiating patch and its radius has been evaluated with the subsequent equations [32, 33] by using different designing parameters. Further, the generated hexagonal patch has been copied and attached to the upper side of another hexagonal patch to obtain the desired dual hexagonal radiating patch shape as reported in Fig. 1(a). A partial ground plane and a 50Ω transmission line feed have been used to excite the designed radiating patch and to obtain the proper impedance matching characteristics. The HFA is designed and investigated by employing the simulator called Ansys HFSS V13 based on the finite element method.

$$R_1 = \frac{F}{\left\{1+\frac{2h}{\pi F \varepsilon_r}\left[\ln\left(\frac{\pi F}{2h}\right)+1.7726\right]\right\}^{\frac{1}{2}}} \quad (1)$$

$$Where, F = \frac{8.791\times10^9}{f_r\sqrt{\varepsilon_r}} \quad (2)$$

Further, the 1st iteration of the hybrid fractal curve (Koch and Meander) is engraved from the outer sides of the dual hexagonal-shaped radiating patch as previously designed to acquire the 1st iteration of the proposed antenna. These designs of the hybrid fractal curves are inspired and taken from [34, 35] and the process of designing and hybridization of these curves are simply omitted here for the sake of easiness. Similarly, the 2nd iteration of these curves introduced on the dual hexagonal-shaped patch to attain the 2nd iteration of designed HFA as depicted in Fig. 1(c). Parametric dimensions of the designed antenna

are tabulated in Table 1. The assessment of the simulated coefficient of reflection response with respect to resonant frequency for every designed iteration is depicted in Fig. 2.

Table 1
Optimal size of HFA

Parameter	S_1	S_2	R_1	R_2	T_1	F_1	F_2	G_1
Size (mm)	20	40	7.2	7.2	0.55	14.05	1.0	13.5

It can be observed from Fig. 2, that the 0th iteration of the antenna exhibits a single frequency band at 6.1GHz with the corresponding coefficient of reflection of -12.24dB and a BW of 770MHz (5.68–6.45GHz). Whereas, 1st iteration of the antenna reveals one more frequency band as compared to the 0th iteration and displays a frequency band at 1.7 (-12.28dB) and 5.2GHz (-17.94dB) with a -10dB impedance BW of 1.07GHz (1.38–2.45GHz) and 1.03GHz (4.76–5.79GHz). Finally, 2nd iteration of the antenna reports the dual-frequency band at 1.7GHz and 5.0GHz with a coefficient of reflection of -14.40dB and − 20.26dB respectively. This antenna reveals the BW of 1.29GHz (1.31–2.6GHz) and 1.01GHz (4.56–5.57GHz). It is evident from the above discussion that modification in the shape of the designed radiating patch plays a vital role in improving the antenna operational parameters in respect of coefficient of reflection, BW, and number of frequency bands. In this sub-section, the hybrid fractal curves up to 2nd iteration are superimposed on the dual hexagonal-shaped radiating patch to investigate the operation of the antenna. Further, the 1st and 2nd iteration of the hybrid curve is employed on the PGP in the next sub-section, which should lead to the enhancement of resonant frequency bands and better impedance matching characteristics.

2.2 Effects of hybrid fractal curve on Partial Ground Plane (PGP)

In this sub-section the 1st iteration of the hybrid fractal curve is employed in the PGP of the 1st iteration of the antenna and designated as Antenna – 1 as shown in Fig. 3(a). Similarly, the 2nd iteration of the hybrid curve is employed on the PGP of the 2nd iteration of the antenna and is called Antenna – 2 (proposed) as illustrated in Fig. 3(b). The coefficient of reflection response of these antennas is compared in Fig. 4. It can be observed from Fig. 4, that the modification in PGP reveals the quad-band frequency response in the required frequency range. After analyzing the frequency response of Antenna – 1, it can be anticipated that it resonates at 1.6, 5.1, 7.4, and 9.6GHz with a corresponding coefficient of reflection of -14.71, -29.66, -14.91, and − 11.58dB. Whereas, Antenna – 2 reveals the resonance points at 1.6, 4.8, 6.9, and 8.8GHz with the corresponding coefficient of reflection of -19.45, -35.92, -23.29, and − 16.27dB. It is also pragmatic that the Antenna – 2 (proposed) divulges enhanced coefficient of reflection and BW at all the frequency points and the resonant frequency of second, third, and fourth band shifts towards the lower side from also shifts from 5.1 to 4.8GHz, 7.4 to 6.9GHz and 9.6 to 8.8GHz which also helps in reducing the overall size of the antenna. The simulated results of the antenna (Antenna – 1 and 2) with modified PGP are compared in Table 2 for better understanding. Due to the enhanced operation, Antenna – 2 acts as a final proposed shape of the antenna and has been fabricated for the authentication of

obtained results. The fabricated prototype and the comparison of measured results for the final shape of the proposed antenna are discussed in detail in the next section.

The current distribution on the plane of the patch and modified ground plane of the final structure of the designed antenna at operational resonant frequency points are plotted and expounded in Fig. 5. It can be predicted from Fig. 5(a) that current is concerted on the PGP loaded with a hybrid fractal curve in conjunction with dual hexagonal-shaped hybrid radiating fractal patch and microstrip transmission line, due to which proposed antenna displays enhanced coefficient of reflection and BW at 1.6GHz in association with the Antenna – I. Further, at other resonant frequency points such as 4.8 and 6.9GHz, the current is largely concerted on the fractal curve edges of the radiating patch as well as on the transmission line, which supports the shifting of frequency bands and improvement in coefficient of reflection. Finally, at the final frequency point as 8.8GHz, the large current will get saturated at the lower edges of radiating patch and at the ground plane in conjunction with line feed which helps to achieve the upgraded coefficient of reflection and BW up to 1.51GHz in comparison to other structure of antenna (Antenna – I) which exhibit only 0.50GHz BW at last frequency band.

Manufactured Model And Test Results

This section premeditates the made-up model of the proposed antenna together with the comparison of simulated and measured results of various operational indicators. The fabricated structure of the antenna has been delineated in Fig. 6 and the assessment of simulated and measured coefficient of reflection is depicted in Fig. 7. It can be seen in Fig. 7, that the measured antenna exhibit all the frequency bands almost similar to the resonant points revealed by the simulated antenna. So, we can say that both the results (simulated and measured) are in a good match with each other. But, small discrepancies have been reported among the simulated and measured results which may have arisen as a result of the manufacturing tolerance such as soldering bumps of SMA connector as well as inappropriate etching of copper and some variations in the physical dimension of the fabricated structure.

The measured proposed antenna displays the operational frequency ranges from 1.10–3.24GHz, 3.93–5.24GHz, 6.57–7.29GHz, and 8.12–9.72GHz with corresponding impedance BW of 2.14, 1.31, 0.72, 1.60GHz. From, these measured results it is evident that proposed HFA can be used for distinct wireless standards such 1800 MHz 2G spectrum of GSM band (1.71–1.88GHz), Aircraft Surveillance (1.09GHz), 3G Cellular Communication Mobile Uplink (1.90–1.98GHz), Advance Wireless Services (2.11–2.15GHz), LTE 2300/LTE 2500 (2.3–2.4GHz/2.5–2.69GHz), RFID (2.4GHz), Wi-Fi (2.4–2.485GHz), Bluetooth (2.4GHz), WiMAX (3.3–3.7GHz), mobile/fixed satellite navigation (6.61–7.04GHz, 8.175–8.215GHz) and aeronautical and radio navigation (9.0–9.5GHz).

Graphical illustration of the variation in the field strength of radio waves in 2D and 3D space has been specified by using the radiation pattern of the antenna. As the patch antennas are radiate normally to the surface of the metallic radiating element, so these patterns are shown in the rectilinear or polar form with a decibel (dB) strength scale. The simulated and measured radiation patterns in E and H-plane at distinct

resonant frequency points are delineated in Fig. 8. Proposed HFA reveals nearly bidirectional in E-plane and completely Omni-directional pattern in H-plane at operative frequency bands, which clearly postulates that the proposed antenna is an appropriate candidate for multiband wireless applications. Peak realized gain and radiation versus frequency are represented in Fig. 9 in the anticipated frequency ranges. This evidently displays that the measured and simulated gain responses are in reasonable congruent with each other. It can also be reported that the gain of the proposed antenna varies between 1.0 to 4.87dB, 4.62 to 5.28dB, 4.98 to 6.85dB, and 4.75 to 6.28dB in the attained operative frequency ranges. Also, the radiation efficiency of the proposed antenna varies from 0.87 to 0.79% in the first frequency range and almost constant between 0.78 to 0.80% in the other three operational frequency ranges.

Table 2
A Comparison of proposed HFA with existing antennas of same category

Reference	Fractal curves	Size of antenna (mm^2)	Resonant frequencies (GHz)	Maximum gain (dB)
[36]	Sierpinski and Meander	700×400	0.89/1.85/2.04	2.1
[37]	Koch and Cantor	25×66	1.9/3.15	4.78
[38]	Koch and Minkowski	45×38.92	4.46/8.78	5.73
[39]	Koch and Minkowski	39.4×48.4	2.45/3.85/4.45	6.8
[40]	Sierpinski Carpet and Gasket	59×29	2.36/4.7	6.1
[41]	Sierpinski gasket and Meander	400×400	0.925/1.85/2.045	—
[42]		34×34	2.44/5.81	10.19
This work	Giuseppe Peano and Cantor Meander and Koch	20×40	1.6/4.8/6.9/8.8	6.85

The comparison of the proposed HFA has been made with the existing antennas of the same category and illustrated in Table 2 for better understanding. It is evident from Table 2, that the proposed HFA is compact in size and exhibits more frequency bands as compared to the other reported antennas. It has also been observed that HFA deliberated in [42] exhibits more gain as demonstrated by proposed HFA, but it projects less number of frequency bands as well as larger in size, in comparison to it. Thus, giving reliable vision to the above conversation, it can be anticipated that the proposed HFA is best amongst the existing HFAs represented in state of art of literature.

Conclusion

A quad-band HFA using Meander and Koch fractal curves on dual hexagonal-shaped radiating patch has been presented in this manuscript. Three iterations of hybrid fractal curves are superimposed and excited

by using 50Ω transmission line feed as well as a partial ground plane. Further, these curves are applied on a partial ground plane to improve the BW and coefficient of reflection of the designed antenna. The proposed antenna with the 2nd iteration of the curve on the partial ground plane and radiating patch reveals four resonant frequency bands 1.6, 4.8, 6.9, and 8.8GHz with an improved coefficient of reflection and impedance BW. The final design of the antenna is manufactured in the lab and tested experimentally, also the results are compared with simulated results and found incongruent with each other. Due to the enhanced operation of the proposed HFA, it can be a suitable candidate for district wireless applications such as 1800 MHz 2G spectrum of GSM band, Aircraft Surveillance, 3G Cellular Communication Mobile Uplink, Advance Wireless Services, LTE 2300/LTE 2500, RFID, Wi-Fi, Bluetooth, WiMAX, mobile/fixed satellite navigation and aeronautical and radio navigation.

Declarations

- The authors have no relevant financial or non-financial interests to disclose.
- The authors have no conflicts of interest to declare that are relevant to the content of this article.
- All authors certify that they have no affiliations with or involvement in any organization or entity with any financial interest or non-financial interest in the subject matter or materials discussed in this manuscript.
- The authors have no financial or proprietary interests in any material discussed in this article.

Authors are responsible for correctness of the statements provided in the manuscript.

References

1. Sharma, N., & Sharma, V. (2017). A journey of antenna from dipole to fractal: A review. *American Society for Eng Edu*, 6(2), 317–351
2. Bhatia, S-S., Sivia, J-S., & Sharma, N. (2018). An optimal design of fractal antenna with modified ground structure for wideband applications. *Wireless Person Commun*, 103, 1977–1991
3. Dwivedi, R-P., & Upadhyay, D. (2015). High gain dual band antenna using fractal geometry for mobile communication.IEEE Int Conf on Signal Process and Integrated Netw;50–55.
4. Singh, J., & Bhatia, S-S. (2015). Design of fractal based microstrip rectangular patch antenna for multiband applications. *IEEE Adv Comput Conf*. Doi: 10.1109/IADCC.2015.7154799
5. Sivia, J-S., Singh, A., & Kamal, T-S. (2013). Design of Sierpinski carpet fractal antenna using artificial neural network. *Int J of Comput App*, 68(8), 5–10
6. Martins, M-D., Laaha, S., Freiberger, E-M., Choi, S., & Fitch, W-T. (2014). How children perceive fractals: Hierarchical self-similarity and cognitive development. *Cognition*, 133, 10–24
7. Singh, S., & Singh, A. (2016). Design and optimization of a modified Sierpinski fractal antenna for broadband applications. *Appl Soft Comput*, 38, 843–850

8. Tripathi, S., Mohan, A., & Yadav, S. (2014). Hexagonal fractal ultra-wideband antenna using Koch geometry with bandwidth enhancement. *IET Microw, Ant and Propag*, 8(18), 1445–1450
9. Sharma, N., & Bhatia, S-S. (2019). Performance enhancement of nested hexagonal ring shaped compact multiband integrated wideband fractal antennas for wireless applications. *Int J of RF and Microw Comut Aided Eng*, 30(3), 1–21
10. Gangwar, K., Gangwar, R-P-S., & Paras (2015). Enhancement of the gain and bandwidth of MPA using Metamaterial Structure. *Int J of Eng Res & Manag Technol*, 2(2), 295–300
11. Shreshtha, S., Lee, S-R., & Choi, D-Y. (2014). A new fractal-based miniaturized dual band patch antenna for RF energy harvesting. *Int J of Ant and Propag*, 805052(2014), 1–9
12. Susila, M., Rao, T-R., & Gupta, A. (2014). A novel fractal antenna design for UWB wireless communications.IEEE Int Microw and RF Conf;118–120.
13. Bhatia, S-S., Kaur, H., & Rana, S-B. (2018). Design of hexagonal antenna using Meander fractal geometry for wideband applications. I-manager's. *J on wireless Commun Netw*, 7(1), 29–39
14. Liu, G., Gu, J., Gao, Z., & Xu, M. (2019). Wideband printed slot antenna using Koch fractal metasurface structure. *Int J of RF and Microw Comput Aided Eng*, 30(3), 1–6
15. Omar, A-A. (2012). Design of ultrawideband coplanar waveguide fed Koch fractal triangular antenna. *Int J of RF and Microw Comput Aided Eng*, 23(2), 1–8
16. Tripathi, S., Mohan, A., & Yadav, S. (2017). A compact UWB Koch fractal antenna for UWB antenna array applications. *Wireless Person Commun*, 92, 1423–1442
17. Salini, J., Natarajamani, S., & Vaitheeswaran, S-M. (2018). Minkowski fractal circularly polarized planar antenna for GPS application. *Procedia Comput Sci*, 143, 66–73
18. Ataeiseresht, R., Ghobadi, C., & Nourinia, J. (2006). A novel analysis of Minkowski fractal microstrip patch antenna. *J of Electromag Waves and App*, 20(8), 1115–1127
19. Kubacki, R., Czyzewski, M., & Laskowski, D. (2018). Minkowski island and crossbar fractal microstrip antennas for broadband applications. *Appl Sci*, 8(334), 1–9
20. Radonic, V., Palmer, K., Stojanovic, G., & Bengin, V-C. (Flexible Sierpinski carpet fractal antenna on a Hilbert slot patterned ground. Int J of Ant and Propag 2012). ; 980916(2012):1–7.
21. Gehani, A., Agnihotri, P., & Pujara, D. (2017). Analysis and synthesis of multiband Sierpinski carpet fractal antenna using hybrid neuro fuzzy model. *Prog In Electromag Res Lett*, 68, 59–65
22. Kaur, N., Sivia, J-S., & Kaur, M. (Design of modified Sierpinski Gasket fractal antenna for C and X-band applications. IEEE Int Conf on MOOC's, Innov and Technol in Edu 2015). ; 248 – 50.
23. Palandoken, M., & Gocen, C. (2019). A modified Hilbert fractal resonator based rectenna design for GSM900 band RF energy harvesting applications. *Int J of RF and Microw Comput Aided Eng*, 29(1), 1–8
24. Kumar, A., & Pharwaha, A-P-S. (2020). Development of a modified Hilbert curve fractal antenna for multiband applications. *IETE J of Res*. Doi: 10.1080/03772063.2020.1772126

25. Murad, N-A., Esa, M., & Yusoff M-F-M, Ali, S-H-A. (2006). Hilbert curve fractal antenna for RFID application.IEEE Int RF and Microw Conf; 182 – 86
26. Pal, G., & Sharma, N. (2016). Novel design of fractal antenna using Giuseppe Peano geometry for wireless applications. *Int J of Comput App*, 150(7), 29–32
27. Kumar, P., & Kaushik, S. (2018). Design and analysis of ultra-wide band Giuseppe Peano fractal antenna at different height level of substrate. *Int J of Eng Trends and Technol*, 61(2), 117–120
28. Oraizi, H., & Hedayati, S. (2012). Circularly polarized multiband microstrip antenna using the square Giuseppe Peano fractals. *IEEE Trans on Ant and Propag*, 60(7), 3466–3470
29. Wang, P., Wen, G-J., Huang, Y-J., & Sun, Y-H. (2012). Compact Meander T-shaped monopole antenna for dual band WLAN applications. *Int J of RF and Microw Comput Aided Eng*, 23(1), 1–7
30. Singh, M., Kumar, N., Dwari, S., & Kala, P. (2019). Metamaterial inspired miniaturized antenna loaded with IDC and Meander line inductor using partial ground plane. *Int J of RF and Microw Comput Aided Eng*, 29(9), 1–10
31. Sallam, M-O., Soliman, E-A., Vandenbosch, G-A-E., & Raedt, W-D. (2012). Novel electrically small Meander line RFID tag antenna. *Int J of RF and Microw Comput Aided Eng*, 23(6), 639–645
32. Sharma, N., & Bhatia, S-S. (2019). Metamaterial inspired fidget spinner shaped antenna based on parasitic split ring resonator for multi standard wireless applications. *J of Electromag Waves and App*, 34(10), 1471–1490
33. Sharma, N., & Bhatia, S-S. (2021). Stubs and slits loaded partial ground plane inspired hexagonal ring-shaped fractal antenna for multiband wireless applications: design and measurement. *Prog In Elecetromag Res C*, 112, 99–111
34. Kumar, Y., & Singh, S. (2015). Quad-band hybrid fractal antenna for wireless applications.IEEE Int Adv Comput Conf (IACC); 730 – 33
35. Kumar, Y., & Singh, S. (2016). Microstrip fed multiband hybrid fractal antenna for wireless applications. *ACES J*, 31(3), 327–332
36. Lizzi, L., & Oliveri, G. (2010). Hybrid design of a fractal-shaped GSM/UMTS antenna. *J Electromag Waves App*, 24(5–6), 707–719
37. Choukiker, Y-K., & Behra, S-K. (2011). Design of wideband fractal antenna with combination of fractal geometries. *IEEE Int Conf Info Commun Sig Proces*. doi:10.1109/ICICS.2011.6174226
38. Sharma, N., & Sharma, V. (2018). A design of microstrip patch antenna using hybrid fractal slot for wideband applications. *Ain Shams Eng J*, 9(4), 2491–2424
39. Sharma, N., Kaur, S., & Dhaliwal, B-S. (2016). A new triple band hybrid fractal boundary antenna. *IEEE Int Conf on Recent Trends in Electronics Information and Commun Technol*. doi: 10.1109/RTEICT.2016.7807953
40. Saluja, N., & Khanna, R. (2013). Design analysis and fabrication of novel coplanar waveguide-fed hybrid fractal-based Broadband antenna. *Int J of Microw and Wirel Technol*, 5(6), 749–752

41. Azaro, R., Debiasi, L., Zeni, E., Benedetti, M., Rocca, P., & Massa, A. (2009). A hybrid prefractal three-band antenna for multi-standard mobile wireless applications. *IEEE Ant and Wirel Propag Lett*, 8, 905–908
42. Kaur, M., & Sivia, J-S. (2019). Giuseppe Peano and Cantor set fractals based miniaturized hybrid fractal antenna for biomedical applications using artificial neural network and firefly algorithm. *Int J RF Microw Comput Aided Eng*, 30(1), 1–11

Figures

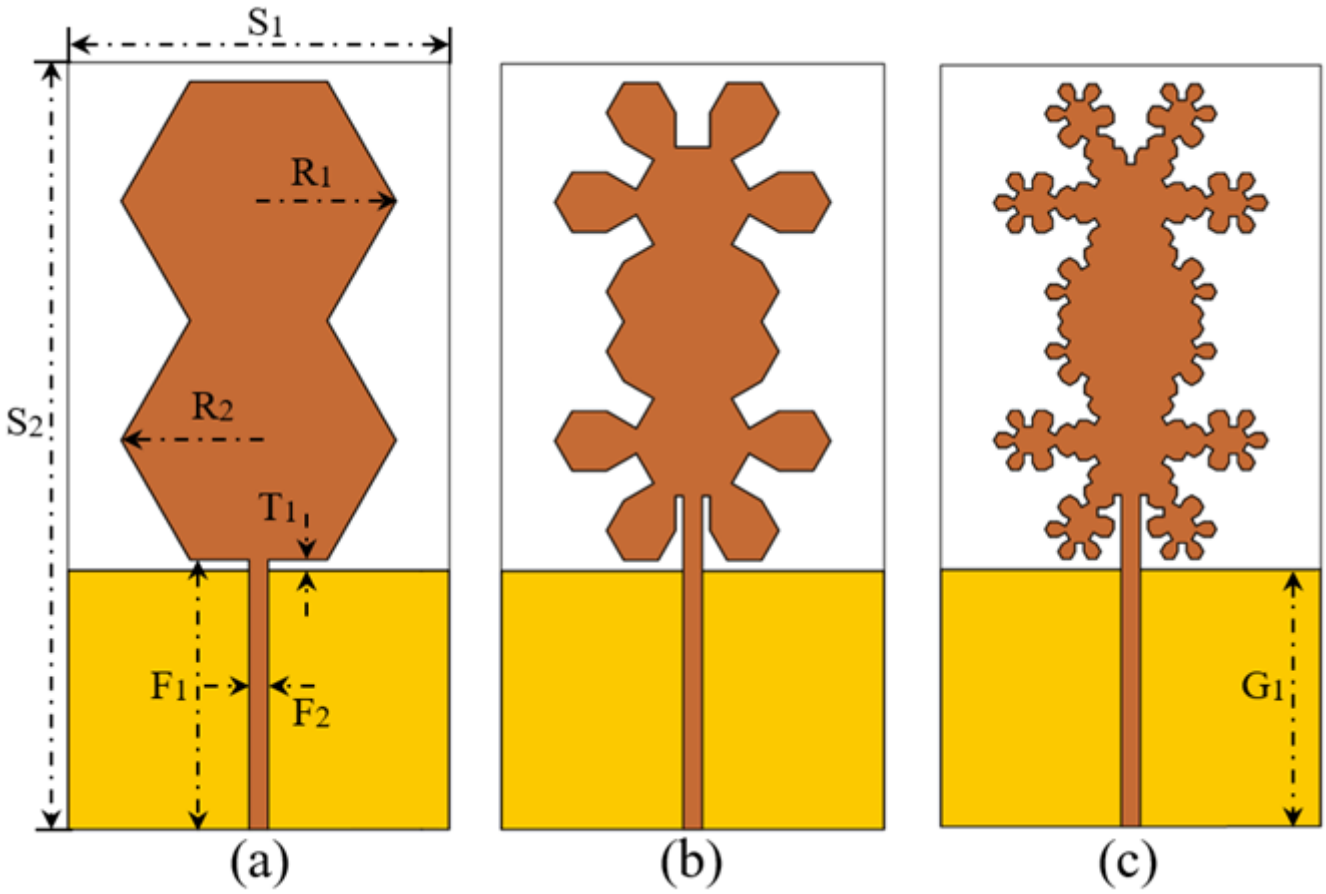

Figure 1

The proposed HFA: (a) 0th (b) 1st and (c) 2nd iterations

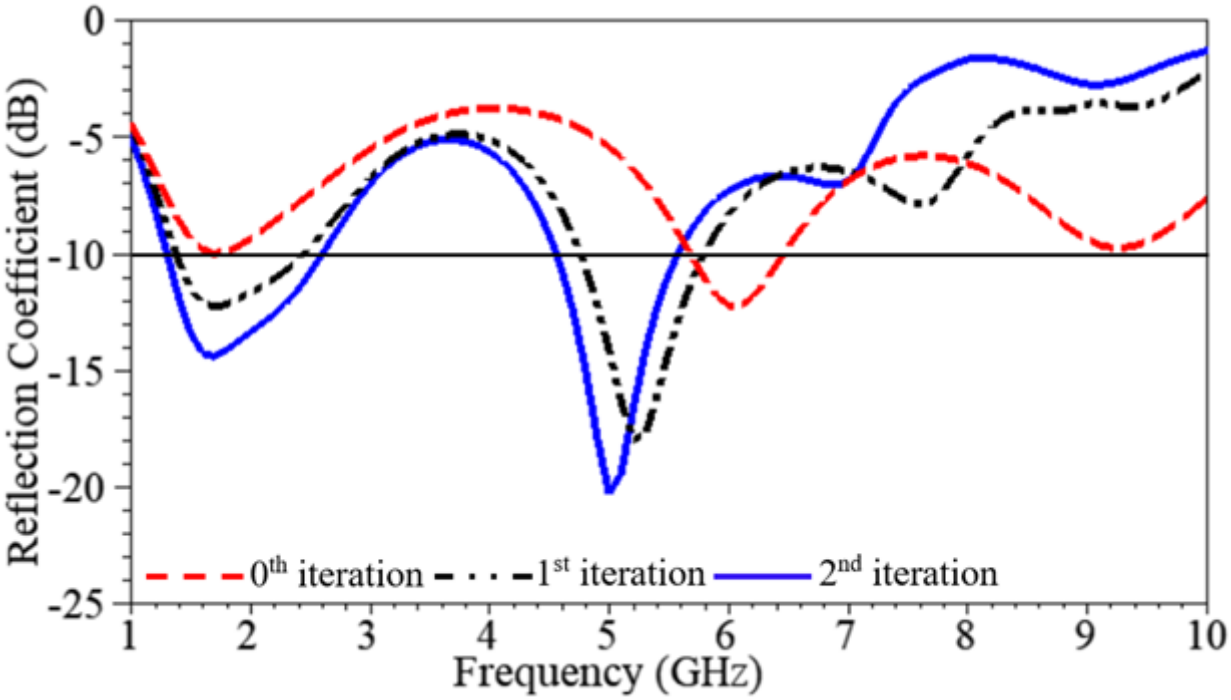

Figure 2

Coefficient of reflection versus frequency plot of HFA

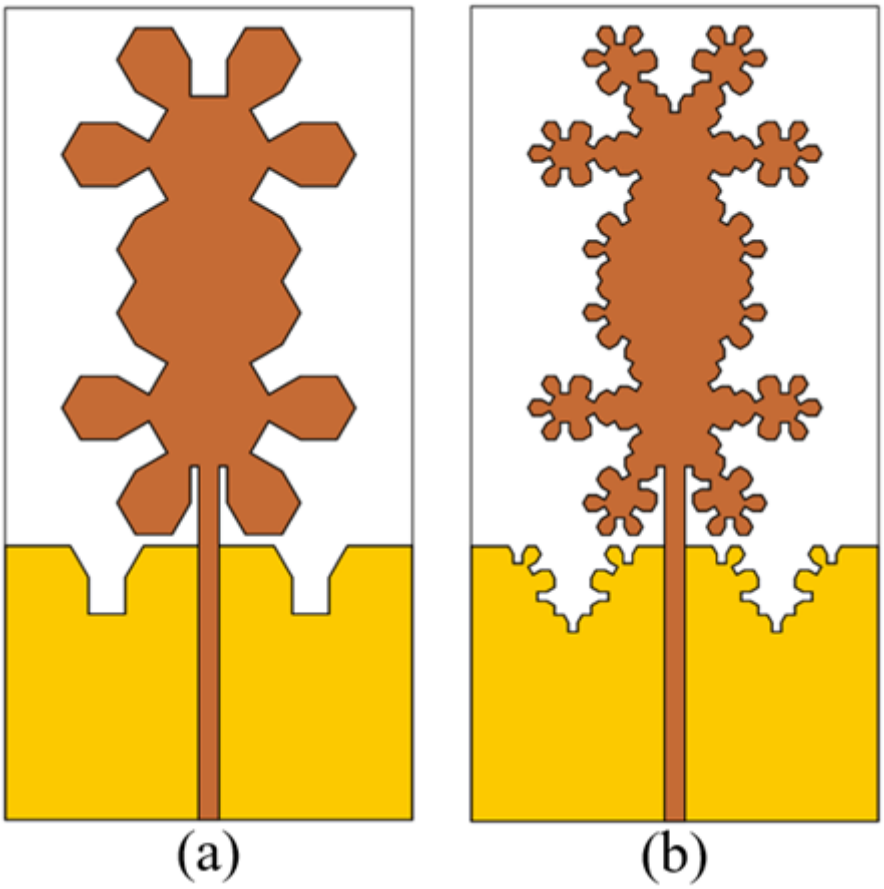

Figure 3

Antenna with modification in PGP: (a) Antenna – 1 and (b) Antenna – 2 (proposed)

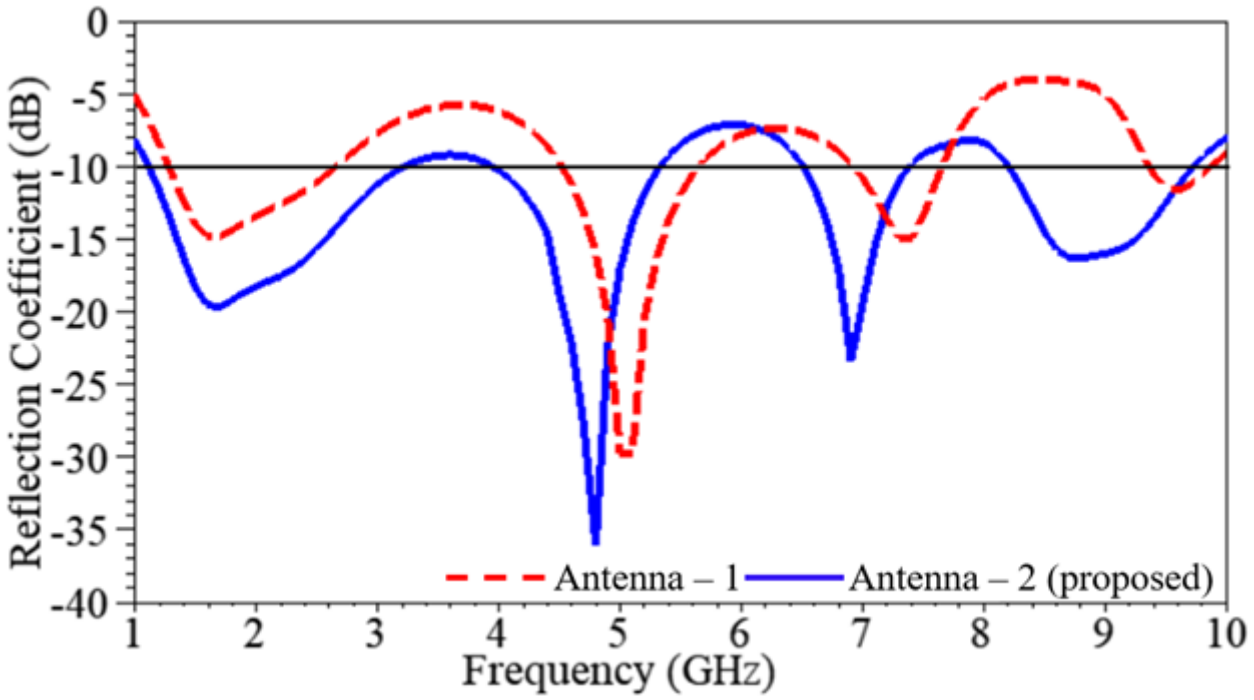

Figure 4

Coefficient of reflection versus frequency plot for HFA with modified PGP

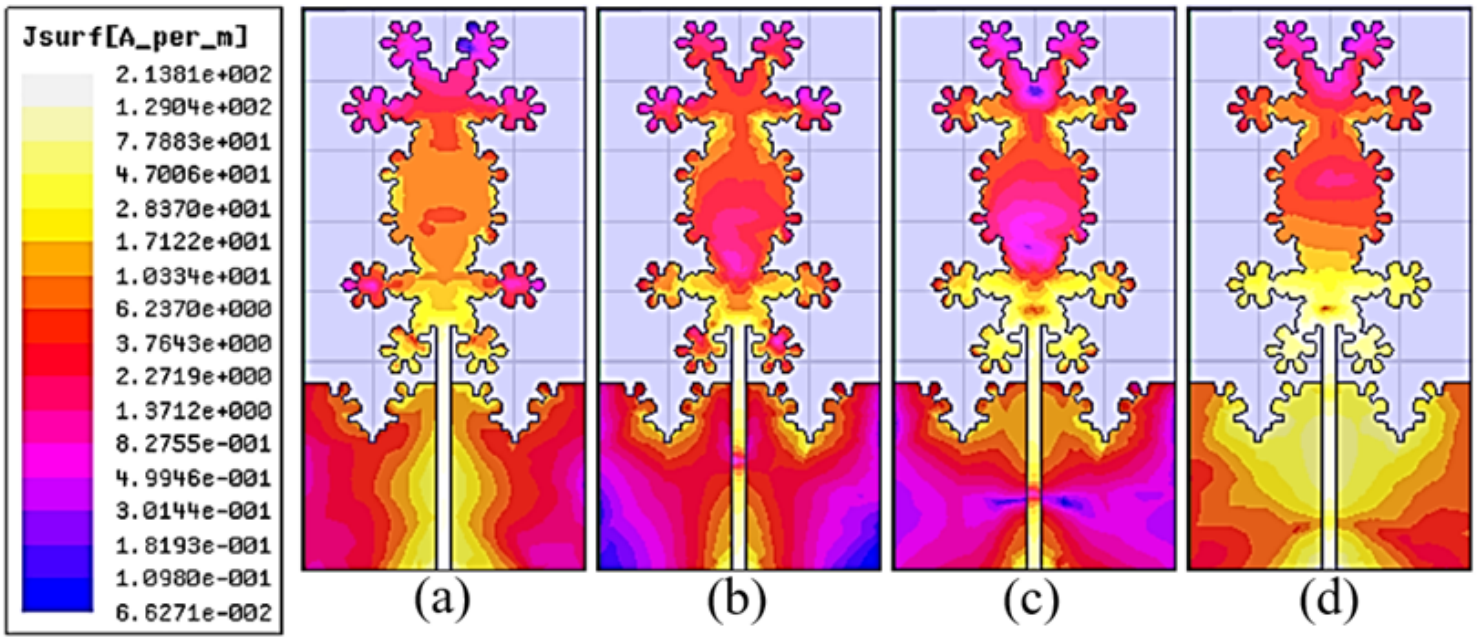

Figure 5

Current distribution plots of the HFA at; (a) 1.6, (b) 4.8, (c) 6.9 and (d) 8.8GHz frequency points

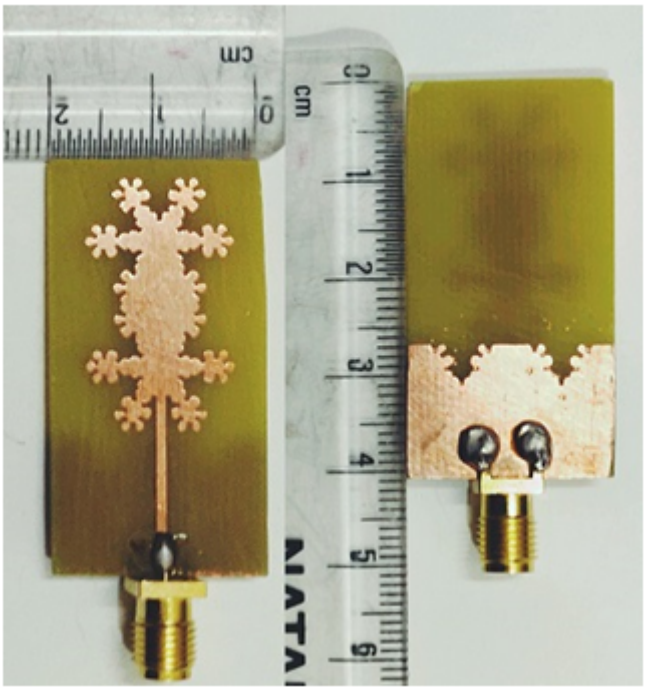

Figure 6

Manufactured model of the HFA

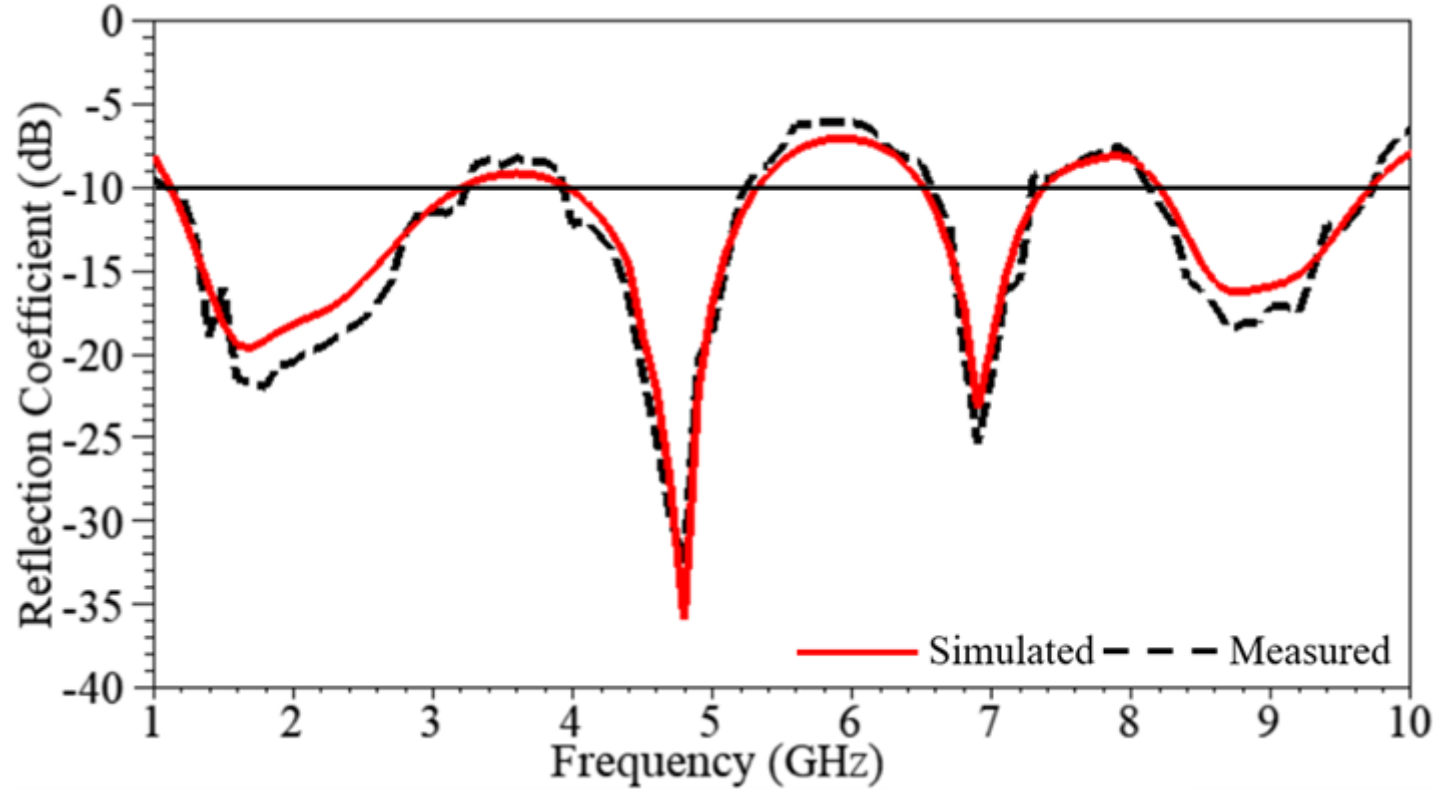

Figure 7

Simulated and measured coefficient of reflection of the HFA

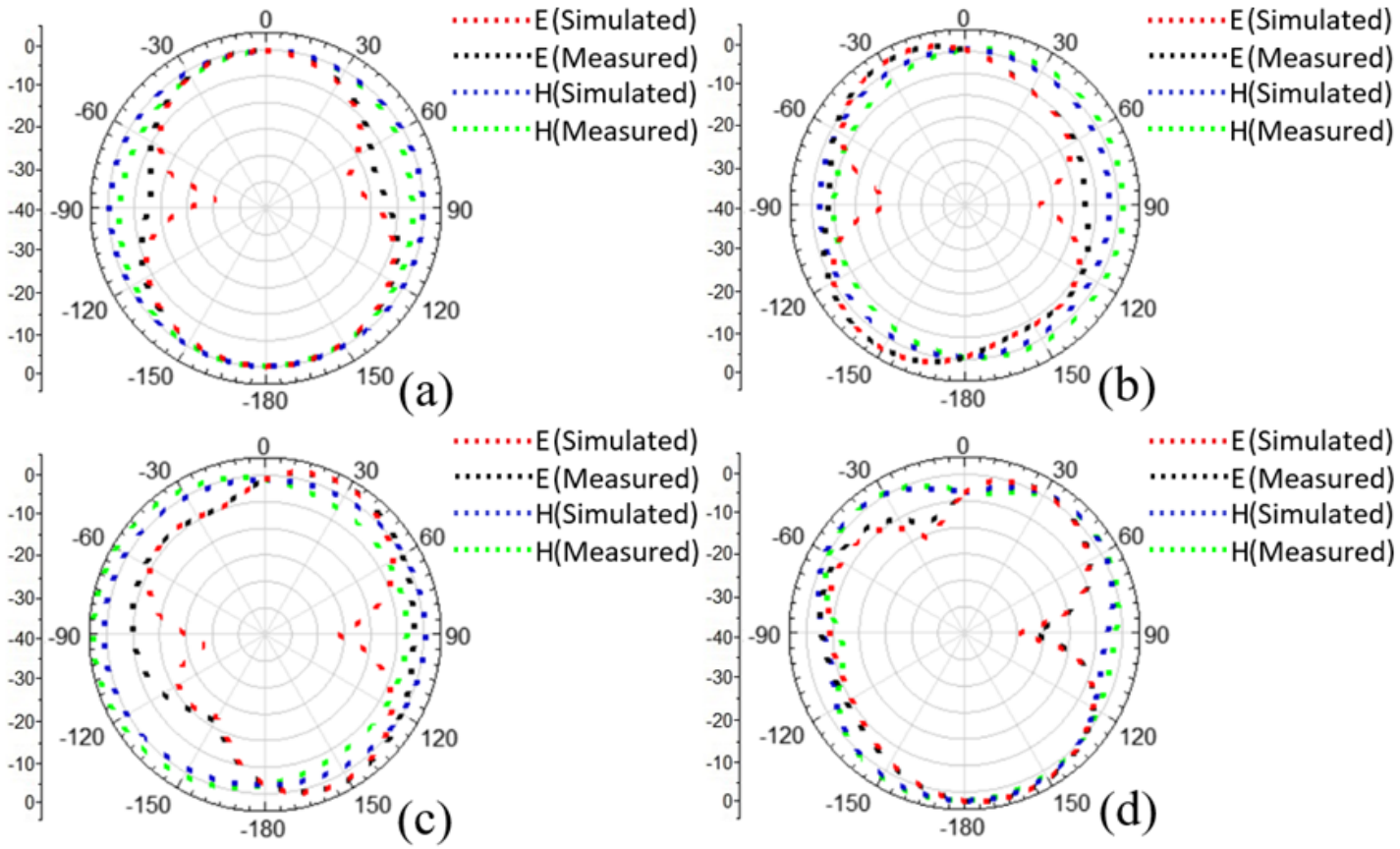

Figure 8

Normalized radiation pattern of the HFA in E and H-plane at (a) 1.6, (b) 4.8, (c) 6.9 and (d) 8.8GHz resonant frequency points

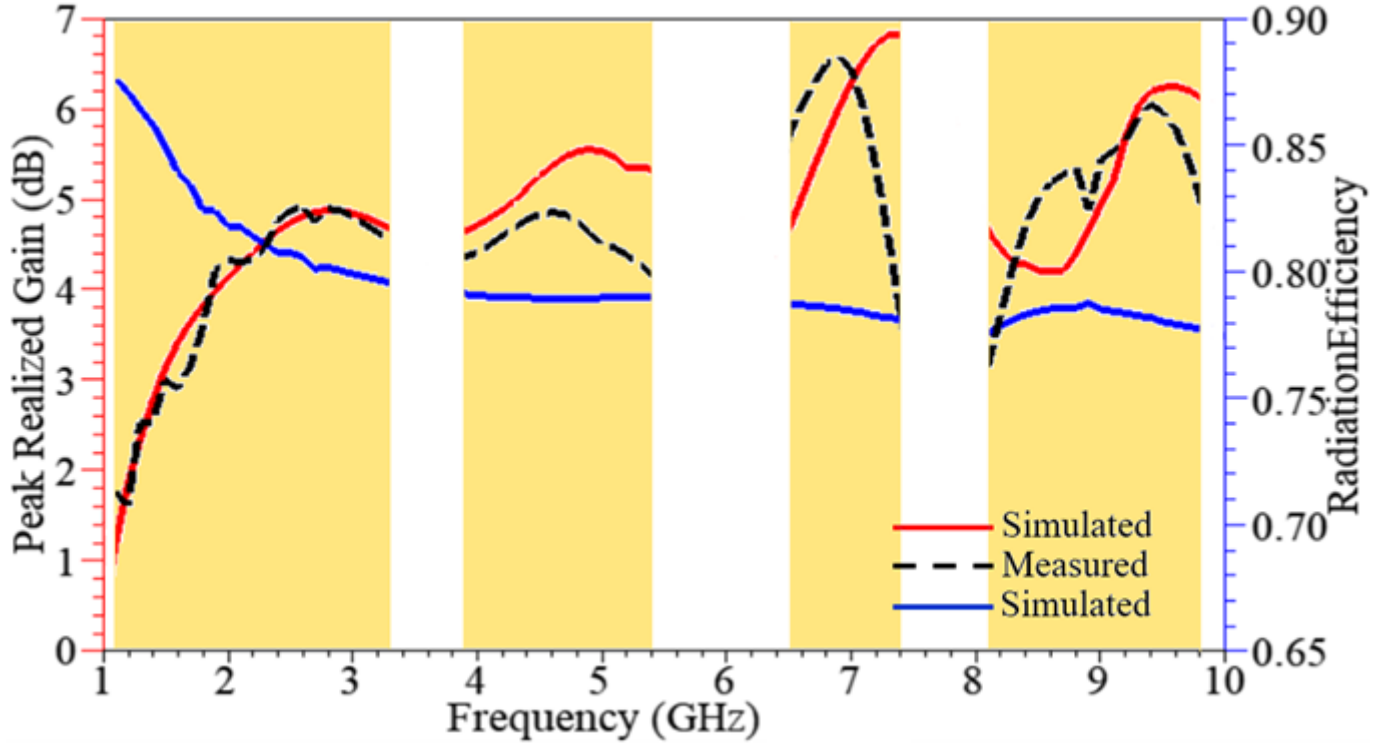

Figure 9

Peak realized gain and radiation efficiency versus freq. plot of HFA